Journal of Organometallic Chemistry, 475 (1994) 73–84

Theoretical study of stable silylenes and germylenes *

Christoph Heinemann [a,1], Wolfgang A. Herrmann [b] and Walter Thiel [a]

[a] *Organisch-chemisches Institut der Universität Zürich, Winterthurerstr. 190, CH-8057 Zürich (Switzerland)*
[b] *Anorganisch-chemisches Institut der Technischen Universität München, Lichtenbergstraße 4, D-85747 Garching (Germany)*

(Received January 13, 1994)

Abstract

Quantum chemical calculations at the semi-empirical, Hartree-Fock and correlated *ab initio* levels have been carried out to rationalize structure, bonding and reactivity of stable cyclic diaminosilylenes and -germylenes. Theory shows excellent agreement with experimental X-ray and electron diffraction data. The calculated thermochemical data provide a consistent description of chemical vapour deposition from a cyclogermylene precursor. Electronic stabilization via p_π–p_π delocalization is an important bonding feature in aminosubstituted silylenes and germylenes. The aminogermylenes have singlet ground states with the lowest triplet states at least 40 kcal/mol higher in energy. In contrast to the homologous aminocarbenes, aminosilylenes and -germylenes are thermodynamically stable with respect to their tetravalent isomers. Planar 2-germaimidazoles are predicted to be unstable. Theoretical data for four different types of Ge–N bonds are compared.

Key words: Silicon; Germanium; Theory

1. Introduction

Recently, the chemistry of stable divalent Group 14 compounds (carbenes, silylenes, germylenes, see Fig. 1) has attracted considerable interest. In 1991 Arduengo and coworkers reported the synthesis and isolation of the first stable carbene of type **4** [1]. The isostructural germylenes **1a** and **2a** have been prepared by Herrmann and coworkers [2] and shown to be promising precursors for the chemical vapour deposition (CVD) of thin germanium layers. Most recently the first stable silylene **3a** has been isolated and characterized by Denk *et al.* [3]. These new compounds have been investigated from the viewpoints of main group [4] and coordination chemistry [5] and by theoretical calculations [6,7].

Extending our earlier work on the stability of aminocarbenes [7] this paper presents a quantum-chemical study of stable aminosilylenes and -germylenes. We first discuss the structures of these molecules, the thermochemistry in the CVD process with aminogermylene precursors, the bonding in the lowest singlet and triplet states, and the singlet-triplet splittings of aminogermylenes. Furthermore, we address 1,2-rearrangements of silylenes and germylenes, and report theoretical results for the lowest singlet and triplet isomers of the composition (Ge, N, H).

2. Computational details

Quantum-chemical calculations were carried out on three levels of theory: (a) within the semi-empirical MNDO and AM1 models; (b) on the *ab initio* Hartree-Fock level (RHF for closed shell systems, ROHF for open shell systems); (c) on various post-Hartree-Fock levels taking account of electron correlation.

Generally, all molecular geometries were totally op-

Correspondence to: Prof. Dr. Walter Thiel.

* Cyclic metalamides, Part IV. For Part III, see: W.A. Herrmann, M. Denk, W. Scherer and F.-R. Klingan, *J. Organomet. Chem.*, *444* (1993) C21.

[1] New address: Institut für Organische Chemie, Technische Universität Berlin, Straße des 17. Juni 135, D-10623 Berlin (Germany).

0022-328X/94/$7.00
SSDI 0022-328X(94)24557-Y

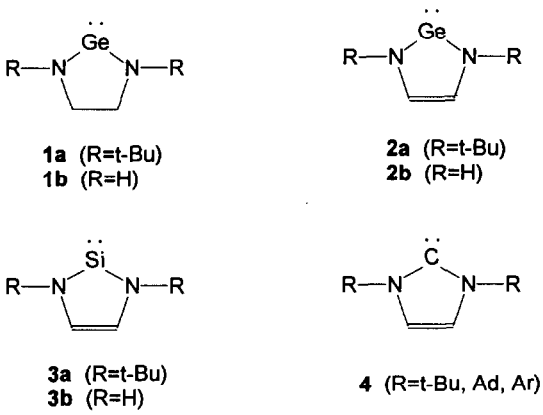

Fig. 1. Cyclic diaminogermylenes, -silylenes and -carbenes investigated in this study.

timized within a given point group using standard gradient techniques. In each case an analysis of the force constant matrix was carried out to verify true minima. Transition states were first located on the semi-empirical MNDO level from the point of maximum energy along a reasonable reaction path. The resulting geometries and force constants then served as starting information for transition state optimizations on the *ab initio* Hartree-Fock level. All transition states were characterized by exactly one negative eigenvalue of the force constant matrix. Unless mentioned otherwise no geometry optimizations were carried out on post-Hartree-Fock levels.

Basis sets of at least double zeta plus polarization (DZP) quality were employed throughout. For carbon, nitrogen and hydrogen the 6-31G* [8] set was used and extended to 6-31G** for the detailed study of $HGeNH_2$ and H_2NGeNH_2, for the 1,2-hydrogen shift reactions and for the calculation of singlet-triplet splittings. The investigation of the (Ge, N, H) energy surface was carried out with triple zeta plus double polarization (TZ2P) basis sets on nitrogen and hydrogen. The (10s6p) and (5s) primitive sets for nitrogen and hydrogen developed by Huzinaga [9] were contracted to [5s3p] and [3s] [10] and augmented by two correlation-consistent polarization functions [11], respectively. All d-polarization functions consisted of five components.

To save computation we replaced the chemically inactive core electrons of germanium and silicon by effective core potentials (ECPs). In most cases the nonrelativistic effective core potentials given by Hay and Wadt [12] were employed (later denoted ECP-1). Germylene singlet-triplet splittings were calculated using the averaged relativistic effective core potential (AREP, later denoted ECP-2) for germanium [13]. In both cases the remaining valence electrons (Ge: $4s^24p^2$, Si: $3s^23p^2$) were treated by the corresponding [12,13] double zeta basis sets ((3s3p)/[2s2p], contraction scheme [21|21]), augmented by one set of d polarization functions with 5 components (exponents: 0.3096, Ge-ECP-1; 0.2979, Ge-ECP-2; 0.4382, Si-ECP-1). The performance of the ECP approach was examined for the 1,2-rearrangement from $H_2Ge{=}NH$ to $HGe{-}NH_2$. On different theoretical levels only small average deviations of 3.1 kcal/mol for the reaction enthalpies and 1.6 kcal/mol for the activation barriers were found when comparing the ECP-1 results to all-electron calculations with a (13s9p7d)/[7s5p4d] basis [14] on germanium.

For the treatment of electron correlation we employed second-, third- and fourth-order Moller-Plesset perturbation theory (MP2, MP3 and MP4, with frozen core), configuration interaction including all single and double excitations (CISD) plus Davidson correction for size-consistency (CISD + Q), and coupled cluster theory with all single and double excitations (CCSD) followed by a perturbational treatment of the triple excitations (CCSD(T)). We use the general notation A/B//C/D to indicate that a certain result was obtained using method A and basis set B at a geometry optimized within method C and basis set D.

The *ab initio* calculations were done using the TURBOMOLE [15] and the GAUSSIAN92 [16] program packages. Semi-empirical calculations were carried out using standard MNDO [17,18] and AM1 [19,20] parameters and our current semi-empirical program [21]. No unusual effects were encountered when employing the recently criticized [22] AM1 parameters for germanium. All programs were run on IBM RS/6000 workstations.

3. Results and discussion

For structural purposes the semi-empirical (MNDO) and pseudopotential/*ab initio* Hartree-Fock methods give very. reasonable descriptions of the divalent germanium and silicon species considered in this study. A comparison of theoretical geometries for cyclogermylenes **1a** and **2a** with the experimental X-ray data [2] shows good agreement (see Table 1). Although this is not surprising it can be taken as an argument that the reported monomeric structures of **1a** and **2a** are not greatly influenced by crystal packing effects. In the refinement of the X-ray data for **1a** [2] a superposition of two C_2-symmetric twist conformers (τ(C–N–Ge–N) = 12.7°) has been assumed to occur in the solid state. Both semi-empirical and *ab initio* calculations agree with this interpretation (*e.g. ab initio*: τ(C–N–Ge–N) = 11.8°). Still there remains the question

TABLE 1. Calculated [a] and experimental [b] structures of **1a** and **2a**

	1a			**2a**		
	MNDO	*ab initio*	exp.	MNDO	*ab initio*	exp.
R(Ge–N)	185.4	183.3	183.3	186.4	185.5	185.6
R(N–C)	145.7	145.8	145.9	141.0	138.4	138.4
R(C–C)	155.8	152.2	157.1	137.1	133.4	136.4
R((CH$_3$)$_3$C–N)	146.8	146.6	146.7	146.9	147.2	149.3
θ(N–Ge–N)	91.2	88.5	88.0	90.0	85.9	84.8
θ(C–N–Ge)	110.9	112.2	113.1	108.3	111.5	113.3
τ(C–N–Ge–N)	6.0	11.8	12.7	0.0	0.0	0.0

[a] Semi-empirical (MNDO) and *ab initio* Hartree-Fock (DZP basis, ECP-1) geometries, bond lengths R in pm, bond angles θ and dihedral angles τ in deg.
[b] X-ray diffraction data, from ref. [2].

whether the two twist conformers are simply disordered or if they interconvert rapidly (Fig. 2).

For this purpose the hydrogen-substituted species **1b** was studied. As the replacement of R = t-Bu by R = H does not dramatically change the electronic nature of the cyclogermylenes the model **1b** is very similar to **1a** in all important structural aspects (*e.g.* for **1b** R(Ge–N): 182.7, MNDO; 182.4 pm, *ab initio*; θ(N–Ge–N): 86.9°, MNDO; 86.2°, *ab initio*). In particular, the dihedral angle characterizing the conformation of the five-membered ring (τ(C–N–Ge–N) = 10.5°, *ab initio*) is nearly the same as in the alkyl-substituted counterpart. If the geometry of **1b** is optimized under the constraint of a planar five-membered ring (C_{2v} symmetry) the resulting bond lengths and angles differ only slightly from those found for the C_2 minimum (*e.g.* R(Ge–N): 182.7, MNDO; 181.7 pm, *ab initio*; θ(N–Ge–N): 86.9°, MNDO; 86.1°, *ab initio*). However, the frequency analysis reveals a saddle point on the potential energy surface (imaginary frequency 117i cm^{-1}, *ab initio*), namely the transition state for the interconversion between the two twist conformations of the five-membered ring. On the Hartree-Fock level the activation energy for this process amounts to 1.3 kcal/mol. The order of magnitude for this barrier suggests that a dynamic exchange between the two conformers of **1a** (see Fig. 2) is possible under the conditions of the X-ray analysis. In the case of the semi-empirical calculations the well known deficiencies of these models correctly to describe conformational degrees of freedom result in very shallow energy profiles for the ring inversion process.

Fig. 2. Ring torsion in aminogermylene **1a**.

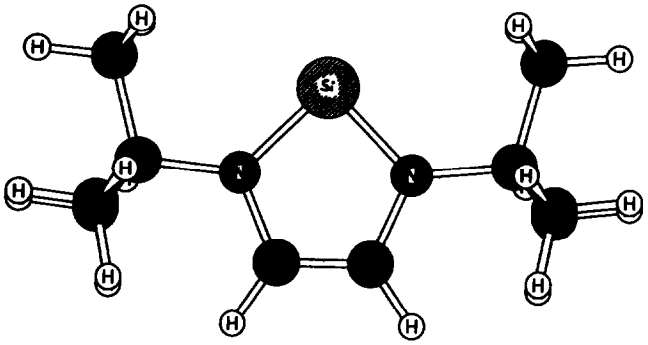

Fig. 3. *Ab initio* structure of the first stable silylene **3a**.

The success of ECP calculations in predicting structural properties of molecules containing electron-rich atoms of higher periods is further exemplified in the case of **3a**, the silicon analogue of cyclogermylene **2a**. The theoretical *ab initio* Hartree-Fock structure is displayed in Fig. 3. Table 2 shows that for all important bond lengths and bond angles the calculated values deviate from the electron-diffraction data [3] by less than 2.5%. The MNDO structure is also in reasonable agreement with the experimental data. The electron diffraction data were refined under C_s symmetry (envelope conformation of the five-membered ring) and indicate a small deviation τ(C–N–Ge–N) = 5(12)°) from a planar five-membered ring. However, both theoretical methods indicate that this molecule has full C_{2v} symmetry (planar five-membered ring) and support the hypothesis [3] that the experimental ring conformation may be due to thermal vibrations.

In view of the potential use of cyclogermylenes as precursors in the chemical vapour deposition (CVD) of thin germanium layers, the thermolysis of **1a** has been studied by photoelectron spectroscopy [2]. A mechanism with two subsequent germanium depositions (first step at $T > 470$ K, second step at T > 900 K, see Fig. 4) was formulated. To rationalize this picture further,

TABLE 2. Calculated [a] and experimental [b] structures of **3a**

	MNDO	*ab initio*	exp.
R(Si–N)	172.8	173.3	173.3
R(N–C$_{sp^2}$)	141.1	139.2	140.0
R(C$_{sp^2}$–C$_{sp^2}$)	137.0	133.0	134.7
R((CH$_3$)$_3$C–N)	146.9	147.5	150.0
θ(N–Si–N)	93.4	89.8	95.5
θ(C$_{sp^2}$–N–Si)	108.8	111.5	110.5
τ(C$_{sp^2}$–N–Si–N)	0.0	0.0	5 (12) [c]

[a] Semi-empirical (MNDO) and *ab initio* Hartree-Fock (DZP basis, ECP-1) geometries, bond lengths R in pm, bond angles θ and dihedral angles τ in deg.
[b] Electron diffraction data, from ref. [3].
[c] See text for discussion.

semi-empirical calculations were carried out to investigate the thermochemistry of this thermolysis. The calculated standard reaction enthalpies (MNDO, AM1) for possible steps of the CVD process are collected in Table 3.

The first step of the thermolysis ($T > 470$ K) can formally be split into two elementary reactions, the dehydrogenation of the germanium precursor **1a** to the C–C unsaturated cyclogermylene **2a** and a reductive cycloreversion of **1a** leading to germanium deposition and the substituted ethylenediamine ligand **5**. The dehydrogenation is endothermic within both semi-empirical models (Δ_rH (MNDO) = 14.6 kcal/mol; $\Delta_r H$ (AM1) = 5.0 kcal/mol). This is compensated by the negative calculated reaction enthalpies for the reductive cycloreversion (**1a** + H_2 → Ge(s) + **5**: $\Delta_r H$ (MNDO) = −17.9 kcal/mol; $\Delta_r H$ (AM1) = −19.3 kcal/mol). Thus the overall reaction in the first step of the thermolysis of **1a** is expected to be exothermic ($\Delta_r H$ (MNDO) = −3.3 kcal/mol; Δ_rH (AM1) = −14.3 kcal/mol). At the end of this step unreacted **1a**, **2a** and **5** are present.

For the second step there are several possible degradation pathways from **1a**, **2a** and **5** to the end products Ge(s), H_2, HCN, isobutene and isobutane

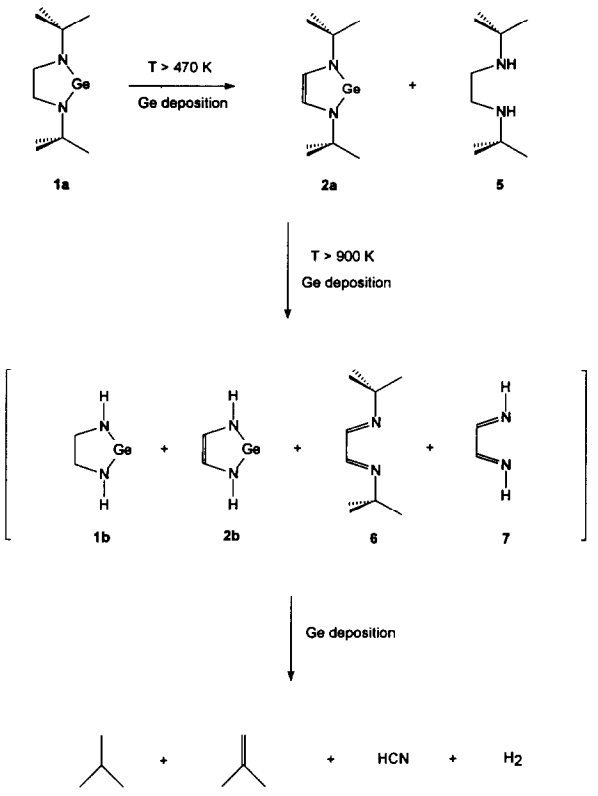

Fig. 4. CVD process for germanium deposition with aminogermylene precursor **1a**.

TABLE 3. Semi-empirical standard reaction enthalpies [a] (kcal/mol) for formal steps in the thermolysis of **1a** [b]

Reaction	$\Delta_r H$ (MNDO)	$\Delta_r H$ (AM1)
First step, T > 470 K		
1a → **2a** + H_2	14.6	5.0
1a + H_2 → Ge(s) + **5**	−17.9	−19.3
2 **1a** → Ge(s) + **2a** + **5**	−3.3	−14.3
Second step, T > 900 K		
1a → **1b** + 2 i-C_4H_8	−5.0	13.6
1a → Ge(s) + 2 HCN + 2 i-C_4H_{10}	11.3	7.8
1a → Ge(s) + 2 HCN + 2 i-C_4H_8 + 2 H_2	62.5	53.8
1b → Ge(s) + 2 HCN + 2 H_2	67.5	40.2
1b → **2b** + H_2	18.5	5.2
2a → **2b** + 2 i-C_4H_8	−1.1	13.8
2a → Ge(s) + **6**	−2.3	11.1
2a → Ge(s) + 2 HCN + H_2 + 2 i-C_4H_8	47.9	48.8
2a → Ge(s) + 2 HCN + i-C_4H_8 + i-C_4H_{10}	22.3	25.8
2b → Ge(s) + **7**	15.5	19.0
2b → Ge(s) + H_2 + 2 HCN	49.0	35.0
5 → 2 HCN + 2 i-C_4H_8 + H_2	79.0	83.4
5 → 2 HCN + i-C_4H_{10} + i-C_4H_8	53.4	60.4
6 → **7** + 2 i-C_4H_8	16.7	21.7
6 → 2 HCN + H_2 + 2 i-C_4H_8	50.2	37.7
7 → 2 HCN + H_2	33.5	16.0

[a] Derived from the following semi-empirical heats of formation (MNDO, AM1): **1a**: 5.7, −4.6; **1b**: 4.5, 11.4; **2a**: 19.6, 5.6; **2b**: 22.3, 21.8; **5**: −11.5, −29.0; **6**: 17.3, 16.7; **7**: 37.8, 40.8; Ge (s): 0.0, 0.0; H_2: 0.7, −5.2; HCN: 35.3, 31.0; i-C_4H_8: −1.9, −1.2; i-C_4H_{10}: −26.8, −29.4. All values in kcal/mol.

[b] See Fig. 4.

which proceed via intermediates **1b** and **2b** (a result of loss of isobutene from the t-butyl substituted cyclogermylenes **1a** and **2a**), and via **6** and **7** (resulting by cycloreversion from the C–C-unsaturated cyclogermylenes **2a** and **2b**). All enthalpy changes for the elementary and overall reactions are positive in AM1, nearly all of them being larger than 10 kcal/mol. The same applies to MNDO, with the exception of three elementary reactions with very low exothermicity (see Table 3). The thermochemistry for the dehydrogenation of the hydrogen-substituted C–C saturated cyclogermylene (**1b** → **2b** + H_2) is nearly the same as for the t-butyl-substituted counterpart **1a** (first step). This implies that bulky substituents do not affect the relative stabilization of the C–C-unsaturated five-membered ring with respect to the C–C-saturated counterpart. The 1,2-hydrogen elimination from 1,2-diaminoethane to *cis*-1,2-diaminoethene ($\Delta_r H$ (MNDO) = 21.9 kcal/mol; $\Delta_r H$ (AM1) = 12.9 kcal/mol) is more endothermic than the dehydrogenations from **1a** and **1b** which indicates a certain stabilization of the cyclic C–C-unsaturated germylenes (**2a**, **2b**). In the case of the corresponding carbenes it has been shown that this stabilization can be interpreted as arising from cyclic π-electron delocalization [7].

Thus, our semi-empirical calculations are consistent with the experimentally deduced two-step nature of the germanium deposition process. The theoretical results indicate that the first step of the thermolysis is driven by its favourable thermochemistry and that the thermal energy at 470 K is necessary only to overcome the relevant activation barriers. The second endothermic step, however, can be regarded as an entropy-driven cracking process that proceeds only at higher temperatures. It has to be stressed that these calculations are not intended to give a final insight into the complex mechanisms under which solid germanium layers can be obtained from precursor **1a** by chemical vapour deposition (CVD). Especially, they apply to pure gas phase reactions and cannot take into account the (catalytic?) role of the Ge-surface and transport mechanisms from the gas phase to the deposition site. Furthermore, we have treated H_2 as a simple CVD-byproduct although in experiments [2] it was found that hydrogen is incorporated into the germanium layers.

To gain further insight into the ability of aminoligands in stabilizing the +II oxidation state in Group 14 compounds a detailed study of the simple models aminogermylene **8** and diaminogermylene **9** was carried out. Table 4 gives an overview of structural and energetic properties for several stationary points (see Fig. 5) on their singlet ground state energy surfaces.

Aminogermylene ($^1A'$) has the planar minimum structure **8a** with a Ge–N distance of 180.0 pm, a Ge–H bond length of 159.0 pm and a typical singlet bond angle θ(N–Ge–H) of 93.1°. Earlier calculations using a different ECP have yielded very similar results [23]. Inclusion of electron correlation (CISD/6-31G**) only results in minor structural changes (R(Ge–N) = 181.2, R(Ge–H) = 160.0 pm, θ(N–Ge–H) = 93.4°). Two transition states (**8b** and **8c**) for rotation around the Ge–N bond with pyramidal nitrogens and different relative orientations of the germanium and nitrogen lone pairs lie close in energy. **8b** with *cis* lone pairs is slightly more stable than **8c** with *trans* lone pairs. The Ge–H bond lengths (161.0, **8b**; 159.5 pm; **8c**) indicate a stabilizing n(N) → σ^*(Ge–H) hyperconjugation in **8b** which is not possible in **8c** and which apparently overcomes any electrostatic preference for **8c** arising from the orientation of the lone pairs. The lowest energy pathway for the inversion at nitrogen (**8b** → **8c**) proceeds via **8d**, a saddle point of order 2 with nearly planar coordination of the nitrogen atom.

The geometries at the nitrogen atom and the unusually high torsional barriers around the formal Ge–N single bond suggest that the unsaturated Ge^{II} centre is stabilized by p_π–p_π electron delocalization from the p_z lone pair at the nitrogen atom into the empty p_z orbital on germanium. Considering **8b** and **8c** as reference structures with true Ge–N single bonds one can deduce that this delocalization shortens the Ge–N bond in **8a** by 8–9 pm. At the CISD + Q/DZP//CISD/DZP level we calculate a rotational barrier of 23.0 kcal/mol which may serve as an estimate of the partial π-bond energy in **8a**.

The effects for diaminogermylene **9** ($^1A_1$) are of the same magnitude. In its planar C_{2v} minimum structure **9a**, p_π–p_π electron delocalization can occur from both nitrogens resulting in a somewhat longer Ge–N bond as compared to **8a**. In a different view the three p_z orbitals form an allyl-type MO system with a doubly occupied bonding (b_1), a doubly occupied nonbonding (a_2) and an empty antibonding (b_1) orbital. Upon rotation around one Ge–N bond the nonrotating bond becomes slightly shorter (**9b**, full delocalization to one side, no hyperconjugation possible) or remains about the same (**9c**, hyperconjugation possible) whereas the rotating bond is lengthened by 6–7 pm. The barrier for rotation around the first bond (**9a** → **9b**: 10.2 kcal/mol, MP4//HF) is less than half of that in aminogermylene **8a** due to the fact that p_π–p_π delocalization can now be established more effectively to the remaining planar nitrogen. However, the barriers for the rotation of the second Ge–N bond (*e.g.* **9b** → **9e**: 21.7 kcal/mol, MP4//HF) are nearly the same as in **8a**.

In the lowest triplet state of aminogermylene **8** the energetic order of the structures found for the singlet

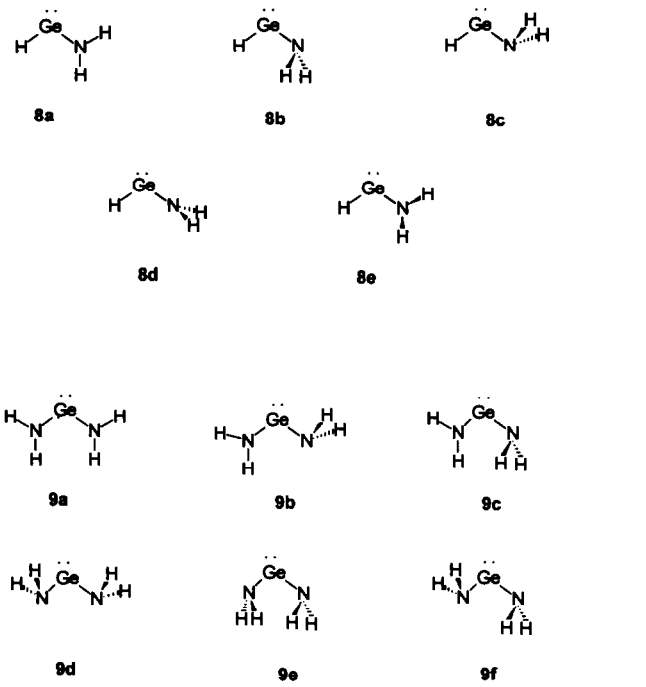

Fig. 5. Stationary points on the lowest singlet and triplet surfaces of aminogermylene **8** and diaminogermylene **9**.

TABLE 4. Geometries, relative energies and imaginary frequencies for stationary points on the lowest singlet energy surfaces of aminogermylene **8** (X = H) and diaminogermylene **9** (X = NH_2) [a]

	Geometries					Relative energies			
	Point group	R(Ge–N)	R(Ge–X)	θ(N–Ge–X)	τ(H–N–Ge–X)	HF	MP2	MP4	ν_{imag}
8a	C_s	180.0	159.0	93.1	0.0	0.0	0.0	0.0	–
8b	C_s	187.9	161.0	99.6	59.6	21.1	24.5	24.1	611i
8c	C_s	188.8	159.5	96.9	121.1	24.0	26.0	25.6	708i
8d	C_s	185.7	160.9	99.1	99.1	24.2	28.7	28.5	513i, 908i
9a	C_{2v}	181.3	181.3	97.9	0.0	0.0	0.0	0.0	–
9b	C_s	179.5	188.9	94.6	0.0, 121.6	11.2	10.7	10.2	377i
9c	C_s	181.1	187.4	99.6	0.0, 59.7	12.2	12.1	11.7	399i
9d	C_{2v}	187.7	187.7	99.5	118.8	34.9	32.9	35.9	566i, 590i
9e	C_{2v}	188.5	188.5	104.2	61.7	30.8	30.4	31.9	448i, 514i
9f	C_s	187.1	189.4	101.4	58.0, 119.6	31.1	30.9	32.1	468i, 527i

[a] Hartree-Fock geometries (DZP basis, ECP-1), bond lengths R in pm, bond angles θ and dihedral angles τ in deg; energies in kcal/mol, frequencies in cm^{-1}.

is reversed (see Table 5). Upon promotion of an electron from the n_σ lone pair into the p_z-orbital on the germanium atom the valence angle θ(H–Ge–N) opens up by more than 20°, which is a common finding for divalent Group 14 species. The planar structure **8a** is characterized as a saddle point of order 2 on the triplet surface. Its imaginary frequencies correspond to eigenvectors that lead to a pyramidalization at nitrogen and a partial rotation around the Ge–N bond. Following the first of these leads to the saddle point **8e**. The true triplet minimum structures **8b** and **8c** lie very close in energy and can interconvert by rotation around the Ge–N single bond via the transition state **8e**. With respect to the singlet ground state the electronic excitation causes increased p-character in the nonbonding hybrid AOs of germanium and higher s-character in those AOs contributing to the σ-bonds. This leads to a decrease of 7–8 pm in the Ge–H distance while the Ge–N bond length remains nearly unaffected since p_π–p_π delocalization is less extensive in the triplet than in the singlet ground state. A lower value for the rotational barrier (8.4 kcal/mol, MP2//HF) is in accord with this interpretation.

The three minimum conformers **9d**, **9e** and **9f** in the lowest triplet state of diaminogermylene lie very close in energy. Qualitatively, their nonplanar structures with pyramidal nitrogens are very similar to those of triplet aminogermylene **8**. Compared to the singlet ground state minimum **9a** the valence angles θ(H–Ge–N) are larger and the Ge–N distances are nearly the same because the loss of p_π–p_π delocalization is compensated by the change of hybridization on the germanium atom.

Due to their application as CVD precursors the singlet-triplet splittings ΔE_{ST} of aminogermylenes such as **1** or **2** are not only of academic interest. For a

TABLE 5. Geometries, relative energies and imaginary frequencies for stationary points on the lowest triplet energy surfaces of aminogermylene **8** (X = H) and diaminogermylene **9** (X = NH_2) [a]

	Geometries					Relative energies		
	Point group	R(Ge–N)	R(Ge–X)	θ(N–Ge–X)	τ(H–N–Ge–X)	HF	MP2	ν_{imag}
8a	C_s	180.5	151.5	115.4	0.0	8.3	11.1	567i, 457i
8b	C_s	179.6	153.1	120.9	75.3	0.4	2.3	–
8c	C_s	181.3	152.6	116.5	112.0	0.0	0.0	–
8e	C_1	183.9	151.9	116.5	21.6, 143.3	6.1	8.4	257i
9d	C_{2v}	181.3	181.3	118.4	114.6	1.7	4.8	–
9e	C_{2v}	182.0	182.0	117.4	69.2	0.0	0.0	–
9f	C_s	181.3	182.9	120.6	67.0, 114.3	0.3	1.6	–

[a] Hartree-Fock geometries (DZP basis, ECP-1), bond lengths R in pm, bond angles θ and dihedral angles τ in deg; energies in kcal/mol, frequencies in cm^{-1}.

TABLE 6. Geometries and relative energies for the lowest singlet ($^1A_1$) and triplet ($^3B_1$) states of GeH_2 obtained with relativistic and nonrelativistic pseudopotentials [a]

	Geometries				Relative energies	
	ECP-1 (nonrel.)		ECP-2 (rel.)		ECP-1 (nonrel.)	ECP-2 (rel.)
	R(Ge–H)	θ(H–Ge–H)	R(Ge–H)	θ(H–Ge–H)		
Singlet state $^1A_1$						
Hartree-Fock	158.5	92.7	157.2	92.7	0.0	0.0
MP2	159.3	91.6	158.2	91.5	0.0	0.0
MCSCF [b]	161.8	92.6	160.6	92.5	0.0	0.0
CISD	160.4	91.4	159.3	91.3	0.0 [c]	0.0 [c]
Triplet state $^3B_1$						
Hartree-Fock	153.3	118.2	151.8	118.8	8.5	11.1
MP2	154.2	118.6	152.9	119.2	16.7	19.0
MCSCF [b]	156.1	118.4	154.0	119.0	20.4	22.4
CISD	155.3	118.5	154.0	119.1	20.2 [c]	22.2 [c]

[a] DZP valence basis sets; bond lengths R in pm, bond angles θ in deg, energies in kcal/mol.
[b] Including all symmetry-adapted configurations obtained by distributing the 6 valence electrons in the H 1s and the Ge 4s and 4p orbitals.
[c] Including Davidson correction, CISD + Q.

detailed understanding of deposition mechanisms it is necessary to know to what extent excited states are involved and if state-specific reactivity must be expected. As no experimental data on singlet-triplet splittings for germylenes are available we have calibrated the level of theory appropriate for this study to a high-level pseudopotential calculation of GeH_2 in which a multireference second-order configuration interaction scheme with explicit inclusion of the relativistic spin-orbit coupling effects (MCSCF-SOCI-RCI) and a basis set of quadruple-zeta quality on germanium (including one f polarization function: QZP) yielded a value of 23.1 kcal/mol for the singlet-triplet splitting [24]. Table 6 summarizes our results obtained with four theoretical methods employing both the nonrelativistic and the relativistic effective core potential in connection with the corresponding DZP valence basis sets. In the following discussion we take the MR-SOCI-RCI value of 23.1 kcal/mol as an "accurate" reference for $\Delta E_{ST}(GeH_2)$. Similar to the carbene case the Hartree-Fock method underestimates the singlet-triplet substantially because a one-determinant wavefunction is only a poor description of the singlet state. While MP2 corrections recover more than half of the correlation correction for $\Delta E_{ST}(GeH_2)$ the MCSCF and the CISD methods give results that deviate less than 1 kcal/mol from the reference value when the relativistic ECP is used. As the CISD/DZP-optimized structures (*e.g.* for the singlet state: R(Ge–H) = 159.3 pm, θ(H–Ge–H = 91.3°) are closer to the reference results (R(Ge–H) = 158.7 pm, θ(H–Ge–H) = 91.5°) than those at the MCSCF level (R(Ge–H) = 160.6 pm, θ(H–Ge–H) = 92.5°) it was decided to calculate the singlet-triplet splittings of the aminogermylenes **1b**, **2b**, **8** and **9** using the relativistic ECP-2 with CISD as the highest level of theory.

The results (see Table 7) follow well-known trends and look similar to those recently reported [7] for the homologous aminocarbenes. Generally, the correlation effects on the singlet-triplet gaps are smaller for the aminogermylenes than for GeH_2 because the main deficiency of a one-determinant description of the singlet state (neglect of the $n_\sigma^0 p_z^2$ contribution) is already partially compensated at the Hartree-Fock level by π-electron donation from the α-substituents. As expected [25], the singlet-triplet splittings increase with the electronegativity of the ligands. Our value of 43.1 kcal/mol (CISD + Q//CISD) for aminogermylene **8** (*ca.* 40 kcal/mol were predicted earlier [23] from the orbital energies of the singlet) is close to the values of 43.3 kcal/mol (MP4//MP2) for GeH(OH) [26] and 39.9 kcal/mol (MR-SDCI) for GeHCl [27]. Substitution of the hydrogen atom by a second amino group leads to a value of 57.9 kcal/mol for diaminogermylene **9** (increase of 16.8, compared to 19.5 kcal/mol in the case of the aminocarbenes [7]). Again, this value is

TABLE 7. Singlet-triplet splittings for aminogermylenes

	HF	MP3	CISD	CISD+Q
1b [a]	63.3	75.5	71.4	75.4
2b [a,c]	75.4	91.5	85.6	91.0
8 [b]	33.2	40.9	40.8	43.1
9 [b]	50.5	58.4	55.6	57.9

[a] Calculated at Hartree-Fock/DZP-optimized geometries.
[b] Calculated at CISD/DZP-optimized geometries.
[c] Triplet state from the $n_\sigma \rightarrow p_z$ excitation; a lower triplet results from the $\pi \rightarrow \pi^*$ excitation at the C–C double bond (see text).

similar to the chlorine analogue $GeCl_2$ (60.3 kcal/mol, MR-SDCI [27]). The further increase by 17.5 kcal/mol in going from diaminogermylene **9** to the cyclic C–C-saturated diaminogermylene **1b** is of a similar magnitude as in the carbon case [7]. This is caused by an extra destabilization of the triplet due to the small N–Ge–N angle in the ring (94.6° for **1b**; 117.4° for **9**).

The lowest triplet state (^3B, 77.2 kcal/mol above the singlet, CISD + Q//HF) of the C–C-unsaturated aminogermylene **2b** arises from a $\pi \rightarrow \pi^*$ excitation at the C–C double bond. The $n_\sigma \rightarrow p_z$ excitation at the germylene centre leads to a second ^3B state, 15.6 kcal/mol (CISD + Q//HF) more destabilized with respect to the singlet ground state than the C–C-saturated germylene **1b**. As in the case of the homologous cyclic aminocarbenes one may interpret this as an indication for a certain degree of cyclic π-electron delocalization in **2b**. However, it has to be taken into account that due to the lower electronegativity of germanium the p_z AOs of this element contribute less to the three occupied π-MOs of the unsaturated ring than those at the carbene centre in the corresponding carbene.

One particular aspect of the stability of the germylenes **1a** and **2a** and of the silylene **3a** is the fact that no 1,2-rearrangements to tetravalent germa- and silaimines have been observed. For the isostructural stable carbenes we have shown [7] that such reactions leading to imidazoles are thermodynamically favourable but hindered by substantial activation barriers. Aminosilylenes and -germylenes (see Figs. 6 and 7) are qualitatively different. Here, the divalent state itself is thermodynamically preferred to tetravalent structures with Si–N or Ge–N double bonds. Tables 8 and 9 show that this is a general result of all quantum chemical methods employed in this study. Our best correlation treatment (CCSD(T)) predicts that silaimine **10**, Z-silaacetamidine **11** and 2-silaimidazole **12** are destabilized with regard to their silylene isomers **13**, **14** and **3b** by 14.2, 19.2 and 31.8 kcal/mol, respectively. For germaimine **15** (isomerization to aminogermylene **8** exothermic by 32.6 kcal/mol, CCSD(T)) and Z-germaacetamidine **16** (isomerization to diaminogermylene **9** exothermic by 40.7 kcal/mol, CCSD(T)) the effects are even more pronounced and point to the well-known empirical rule that the stability of low oxidation states increases along a main group of the periodic table.

Unexpected results were obtained in the case of the cyclic diaminogermylene **2b** (see Fig. 7). In contrast to

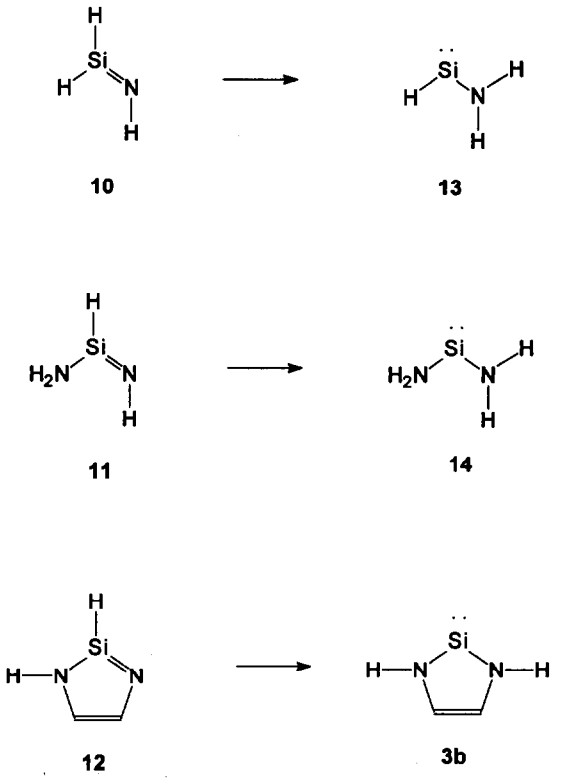

Fig. 6. 1,2-hydrogen shifts from silaimines to aminosilylenes.

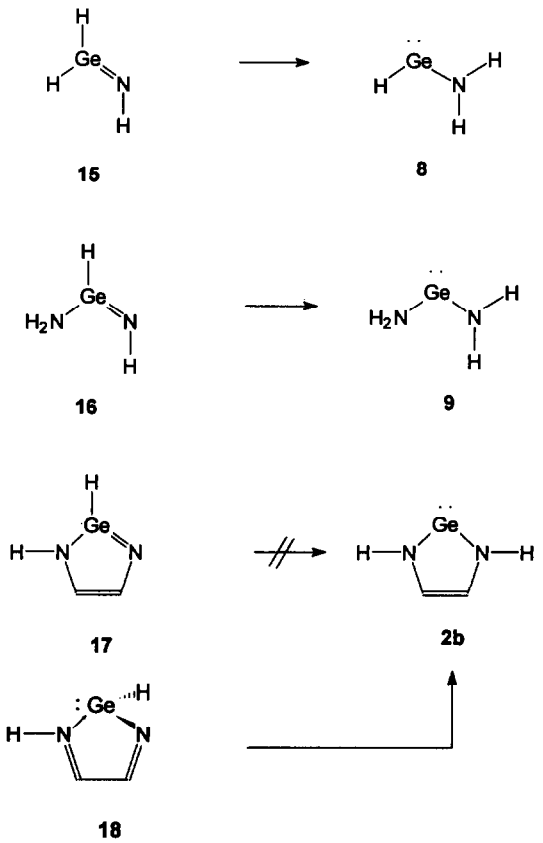

Fig. 7. 1,2-hydrogen shifts to aminogermylenes.

TABLE 8. Reaction energies ΔE_{rct} and barriers ΔE_{act} for 1,2-H-shifts to aminosilylenes (in kcal/mol)

	10 → 13	11 → 14	12 → 3b
ΔE_{rct}			
MNDO	−13.3	−34.5	−23.2
HF	−17.9	−19.9	−33.4
MP2	−11.4	−16.3	−28.9
MP3	−15.8 [a]	−21.4	−33.2
CISD	−15.5	−19.4	−32.7
CISD+Q	−14.8	−19.6	−32.3
CCSD	−15.4	−20.0	−33.0
CCSD(T)	−14.2	−19.2	−31.8
ΔE_{act}			
MNDO	62.8	53.5	49.6
HF	68.3	69.0	29.3
MP2	61.0	54.7	27.0
MP3	58.5	54.3	25.3
CISD	60.7	59.9	28.0
CISD+Q	55.5	52.9	24.6
CCSD	56.9	53.5	24.3
CCSD(T)	54.6	50.8	22.6

[a] MP4/6-31G*//HF/3-21G*: −20.2 kcal/mol [33].

the carbon and silicon homologues a true minimum for a planar 2-germaimidazol **17**, the hypothetical 1,2-shift isomer of **2b**, could neither be located on the semi-empirical MNDO nor at the *ab initio* Hartree-Fock level. Under C_s-symmetry the energy surface of this heterocycle is repulsive with regard to the formal Ge–N single bond. Therefore we conclude that the synthesis of planar 2-germaimidazoles appears to be very unlikely. If one allows for relaxation of the geometry without any symmetry constraints the nonplanar structure **18** is found. However, **18** is not a nonplanar 2-germaimidazole. From its geometry (R(Ge–N) = 192.0, 211.9 pm; θ(H–Ge–N) = 94.9°, HF/DZP) it is best considered as a monoiminogermylene, stabilized by intramolecular electron donation from the lone pair of the remote second nitrogen atom into the vacant p_z-orbital. This intramolecular saturation of the electron deficient germylene centre is the stereoelectronic reason for the nonplanar conformation of this molecule. Overall, this once again indicates the strong preference for the divalent *vs.* the tetravalent bonding situation for Ge/N-species. The results in Table 9 indicate that **18** (one donor-substituent in α-position plus intramolecular coordination of a second donor) is much less stable (by 37.4 kcal/mol, CCSD(T)), than its cyclic diaminogermylene isomer **2b** (two donor-substituents in α-position).

In all acyclic cases the activation barriers for the 1,2-hydrogen-shifts in the thermodynamically favourable direction (imines → ylidenes) are higher than 40 kcal/mol (see Tables 8 and 9). Upon improvement of the correlation treatment they converge to the CCSD(T) values of 54.6 (**10** → **13**), 50.8 (**11** → **14**), 45.2 (**15** → **8**) and 40.6 kcal/mol (**16** → **9**). These results are in accord with the preparative isolation of stable silaimines [28] and germaimines [29] at room temperature. In all transient structures the migrating hydrogen has left the molecular plane and is in nearly the same distance from the silicon atom (**10** → **13**: 151.6, **11** → **14**: 149.8 pm) or the germanium atom (**15** → **8**: 160.9; **16** → **9**: 160.9 pm), respectively. The Si–N (**10** → **13**: 161.8; **11** → **14**: 161.5 pm) and Ge–N (**15** → **8**: 173.4; **16** → **9**: 173.3 pm) distances indicate an intermediate location of the transition states on the reaction path between the imine educts (**10**: 154.4; **11**: 156.3; **15**: 167.2; **16**: 166.2 pm) and ylidene products (**13**: 167.1; **14**: 168.5; **8**: 180.0; **9**: 181.3 pm). For the 2-silaimidazole **12** → 2-silaimidazole-2-ylidene **3b** rearrangement the calculated activation energies (*e.g.* 22.6 kcal/mol, CCSD(T)) are substantially lower than for the acyclic silaimines. This suggests a novel synthetic approach to stable cyclic aminosilylenes via 1,2-rearrangements of 2-silaimidazoles.

Related species with Ge=E double bonds (E = C, Si, Ge), their divalent isomers and the connecting transition states have recently been studied by Grev and Schaefer [30]. Our results agree with their finding that a Ge–H distance of *ca.* 162 pm is common to the transition states of such 1,2-hydrogen shifts. Furthermore, these authors report that in the sequence $H_2Ge{=}GeH_2 \rightarrow H_3Ge{-}Ge{-}H$ ($\Delta E_{rct} = 1.7$, $\Delta E_{act} = 14.0$ kcal/mol; CCSD(T)/DZP), $H_2Si{=}GeH_2 \rightarrow$

TABLE 9. Reaction energies ΔE_{rct} and barriers ΔE_{act} for 1,2-H-shifts to aminogermylenes (in kcal/mol)

	15 → 8	16 → 9	18 → 2b
ΔE_{rct}			
MNDO	−38.2	−51.3	−42.0
HF	−41.5	−46.3	−34.1
MP2	−30.9	−38.4	−42.2
MP3	−36.1	−43.6	−39.9
CISD	−36.2 [a]	−43.5	−38.9
CISD+Q	−34.0	−41.9	−37.8
CCSD	−34.8	−42.2	−38.0
CCSD(T)	−32.6	−40.7	−37.4
ΔE_{act}			
MNDO	50.2	43.4	32.7
HF	56.2	58.4	27.2
MP2	53.9	47.5	14.5
MP3	49.3	45.4	18.6
CISD	50.8	50.9	21.7
CISD+Q	45.7	43.2	19.0
CCSD	47.2	43.7	19.1
CCSD(T)	45.2	40.6	16.9

[a] −32.0 kcal/mol from an earlier CI calculation using a different ECP [23].

$H_3Si-Ge-H$ ($\Delta E_{rct} = -3.7$, $\Delta E_{act} = 15.7$ kcal/mol; CCSD(T)/DZP), $H_2C{=}GeH_2 \rightarrow H_3C-Ge-H$ ($\Delta E_{rct} = -13.0$, $\Delta E_{act} = 34.3$ kcal/mol; CCSD(T)/DZP) the activation barriers increase with the exothermicities of the rearrangements. Our CCSD(T)/DZP results for $H_2Ge{=}NH \rightarrow HGeNH_2$ ($\Delta E_{rct} = -32.6$ kcal/mol, $\Delta E_{act} = 45.2$ kcal/mol) match this general trend.

As a common measure [31] for the π-bond energy of the Ge=N double bond in germaimine $H_2Ge{=}NH$ we have calculated the excitation energy to its lowest triplet state. A value of 34.0 kcal/mol is obtained on the CISD + Q/DZP//CISD/DZP level of theory. Comparing this result to the corresponding values for Ge=Ge, Ge=Si and Ge=C double bonds (25, 25 and 31 kcal/mol [32]) it appears that the height of the 1,2-hydrogen-shift barrier is related to the strength of the π component in the doubly bonded educt.

In addition to the different types of Ge–N single and double bonds discussed so far we have performed calculations on the simplest molecules containing formal triple bonds between germanium and nitrogen, HGeN and its tautomer GeNH. Apart from the general theoretical interest in multiple bonds involving elements of higher periods, the species of the composition (Ge, N, H) must be considered as possible intermediates in CVD processes with aminogermylene precursors. Lighter homologues of the compositions (C, N, H) and (Si, N, H) are important species in interstellar chemistry [34].

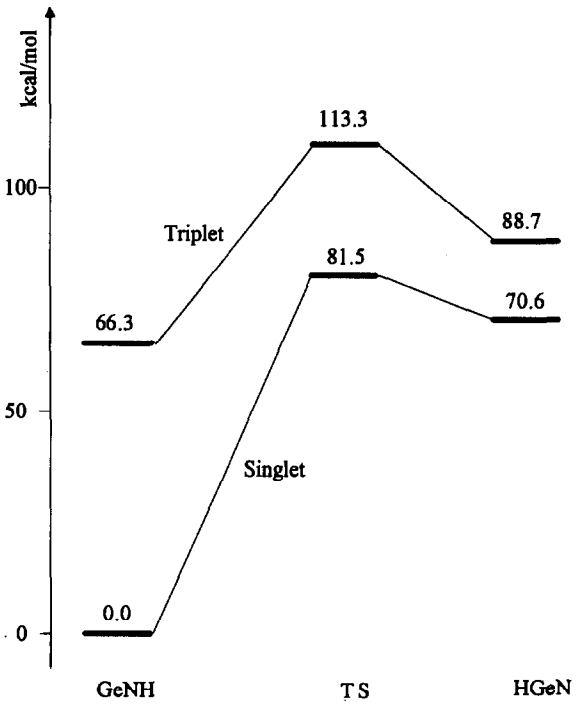

Fig. 8. Relative energies of the lowest singlet and triplet states of GeNH, HGeN and the transition state (TS) for their interconversion.

TABLE 10. Theoretical results for singlet and triplet HGeN and GeNH species [a]

	HGeN	TS	GeNH
Singlet state $^1\Sigma^+$			
$E_{rel.}$	70.6	81.5	0.0
R(Ge–N)	163.8	171.2	164.1
R(Ge–H)	152.5	156.9	
R(N–H)		235.4	99.4
θ(H–Ge–N)	180.0	91.6	0.0
Triplet state $^3A'$			
$E_{rel.}$	88.7	113.3	66.3
R(Ge–N)	177.6	179.0	185.0
R(Ge–H)	159.2	164.5	
R(N–H)		146.2	100.8
θ(H–Ge–N)	98.6	50.3	13.8 [b]

[a] Relative energies in kcal/mol, bond lengths in pm, angles θ in deg. All geometries are optimized at the CISD level, energies include size-consistency correction (CISD + Q).
[b] θ(H–N–Ge): 140.0°.

Figure 8 displays the energies of several stationary points on the lowest singlet and triplet surfaces. All theoretical results are summarized in Table 10. Overall, the singlet state is clearly favoured with respect to the triplet. Similar to the silicon case [35,36] the isomer with central nitrogen, GeNH, represents the global minimum, 70.6 kcal/mol lower in energy than the HGeN species. A substantial shortening in the Ge–N distance in comparison to the formal Ge–N double bond in germaimine **15** ($R(H_2Ge-NH) = 169.8$ pm, CISD) indicates a triple bond between germanium and nitrogen in HGeN ($R(HGe-N) = 163.8$ pm). Interestingly, the position of the hydrogen does not affect the Ge–N distance ($R(Ge-NH) = 164.1$ pm). While a similar situation is found experimentally [37] and theoretically [38] for HCN and CNH this constitutes an important difference from the lighter silicon homologues for which different theoretical methods predict R(HSi–N) to be 6 pm smaller than R(Si–NH) [35,36].

Both linear singlet isomers show a relatively flat energy profile along the angle coordinate [39]. A degenerate pair of π-orbitals (orbital energies: −9.8 eV, HGeN; −10.3 eV, GeNH) lies highest in energy, followed by the mainly nonbonding lone pairs on nitrogen and germanium, respectively (−12.1, HGeN; −11.5 eV, GeNH). The isomerization of HGeN to GeNH proceeds via a rectangular transition state in which the Ge–N distance of 171.2 pm indicates a Ge–N double bond. From the relatively small change in the Ge–H distance (156.9 pm) with respect to HGeN this can be characterized as an "early" transition state, in agreement with the Hammond postulate [40]. Contrary to

the HCN → HNC rearrangement, a relatively low barrier (10.5 kcal/mol, CISD + Q) is found for HGeN → GeNH similar to the HSiN → SiNH case (7.8 kcal/mol, G-1 theory [36]).

The triplet isomers favour nonlinear geometries. Again, the terminal germanium position is preferred, but to a smaller extent (22.4 kcal/mol) than for the singlet species. Different bonding situations can be inferred from the Ge–N distances. In GeNH (R(Ge–NH) = 185.0 pm) the two heavy atoms are connected by a single bond without additional p_π–p_π-delocalization. According to a Mulliken population analysis one unpaired electron resides on Ge and N. In the HGeN tautomer the spin density is mainly located on the nitrogen atom. Thus, this species is best regarded as a singlet germylene bearing one hydrogen and one triplet nitrene substituent which acts as an additional π-donor. In accord with this view, the H–Ge–N angle (98.6°), the Ge–N distance (177.6 pm) and the Ge–H distance (159.2 pm) are close to the typical values for singlet aminogermylenes (*e.g.* 93.4°, 181.2 and 160.0 pm for **8a** on the same level of theory). Finally, the barrier for the 1,2-hydrogen shift from triplet HGeN to triplet GeNH (24.6 kcal/mol) is more than twice the value found for the singlet species.

As an overview Table 11 summarizes the theoretical results for the 4 different types of Ge–N bonds considered in this study. True Ge–N single bonds with distances of 188–189 pm can be found in the rotational transition states **8b** and **8c** of aminogermylene. In the planar minimum structure **8a** of aminogermylene, p_π–p_π delocalisation shortens the Ge–N single bond by about 8–9 pm. The prototypical Ge=N double bond in germaimine **15** is substantially shorter, by 12 pm compared with **8a**. The introduction of a second π bond in HGeN reduces the GeN bond length further, by about 5–6 pm, but significantly less so than the introduction of the first π bond (see above). Judging from the rotational barrier in **8a**, p_π–p_π delocalisation leads to a considerable stabilisation of the order of 20 kcal/mol in aminogermylene. By comparison, the π-bond energy in germaimine **15** (approximated [31] by the $\pi \rightarrow \pi^*$ excitation energy, 34.0 kcal/mol) is not much higher.

TABLE 11. Overview of theoretical results for 4 different Ge–N bond types [a]

Bond type	Model	*R*(HF)	*R*(CISD)	π-bond energy
σ single bond	**8b**	187.9	189.2	
σ single bond plus p_π–p_π delocalisation	**8a**	180.0	181.2	23.1 [a]
$\sigma + \pi$ double bond	**15**	167.2	169.8	34.0 [b]
$\sigma + \pi + \pi$ triple bond	HGeN	162.1	164.0	

[a] From rotational barrier **8a** → **8b**(CISD + Q).
[b] $\pi \rightarrow \pi^*$ excitation energy (CISD + Q).

Acknowledgements

This work was supported by the Alfred-Krupp-Stiftung and the Studienstiftung des deutschen Volkes. We thank Dr. M. Denk for making the manuscript [3] available prior to publication.

References

1 A.J. Arduengo, R.L. Harlow and M. Kline, *J. Am. Chem. Soc., 113* (1991) 361.
2 W.A. Herrmann, M. Denk, J. Behm, W. Scherer, F.R. Klingan, H. Bock, B. Solouki and M. Wagner, *Angew. Chem., 104* (1992) 1489; *Angew. Chem. Int. Ed. Engl., 31* (1992) 1485.
3 M. Denk, R. Lennon, R. Hayashi, R. West, A.V. Belyakov, H.P. Verne, A. Haaland, M. Wagner and N. Metzler, submitted for publication.
4 A.J. Arduengo, H.V. Rasika Dias, J.C. Calabrese and F. Davidson, *J. Am. Chem. Soc., 114* (1992) 9724; A.J. Arduengo, H.V. Rasika Dias, J.C. Calabrese and F. Davidson *Inorg. Chem., 32* (1993) 1541.
5 K. Öfele, W.A. Herrmann, D. Mihalios, M. Elison, E. Herdtweck, W. Scherer and J. Mink, *J. Organomet. Chem., 459* (1993) 177.
6 D.A. Dixon and A.J. Arduengo, *J. Phys. Chem., 95* (1991) 4180.
7 C. Heinemann and W. Thiel, *Chem. Phys. Lett., 217* (1994) 11.
8 W.J. Hehre, R. Ditchfield and J.A. Pople, *J. Chem. Phys., 56* (1972) 2257; P.C. Hariharan and J.A. Pople, *Theor. Chim. Acta, 28* (1973) 213. M.M. Franci, W.J. Pietro, W.J. Hehre, J.S. Binkley, D.J. DeFrees and J.A. Pople, *J. Chem. Phys., 77* (1982) 3654.
9 S. Huzinaga, *J. Chem. Phys., 42* (1965) 1293.
10 T.H. Dunning, *J. Chem. Phys., 55* (1971) 716.
11 T.H. Dunning, *J. Chem. Phys., 90* (1990) 1007.
12 W.R. Wadt and P.J. Hay, *J. Chem. Phys., 82* (1985) 284.
13 M.M. Hurley, L.F. Pacios, P.A. Christiansen, R.B. Ross and W.C. Ermler, *J. Chem. Phys., 84* (1986) 6840.
14 (13s9p5d)/[7s5p2d] set from: R. Poirier (ed.), *Handbook of Gaussian Basis Sets,* Elsevier, Amsterdam, 1985; augmentation by 2d polarization functions from: S. Huzinaga (ed.), *Gaussian Basis Sets for Molecular Calculations*, Elsevier, Amsterdam, 1985.
15 R. Ahlrichs, M. Bär, M. Häser, H. Horn and C. Kölmel, *Chem. Phys. Lett., 162* (1989) 165.
16 M.J. Frisch, G.W. Trucks, M. Head-Gordon, P.M.W. Gill, M.W. Wong, J.B. Foresman, B.G. Johnson, H.B. Schlegel, M.A. Robb, E.S. Replogle, R. Gomperts, J.L. Anders, K. Raghavachari, J.S. Binkley, C. Gonzalez, R.L. Martin, D.J. Fox, D.J. DeFrees, J. Baker, J.J.P. Stewart and J.A. Pople, GAUSSIAN 92, Gaussian Inc., Pittsburgh, PA, USA, 1992.
17 M.J.S. Dewar and W. Thiel, *J. Am. Chem. Soc., 99* (1977) 4899.
18 Ge-parameters: M.J.S. Dewar, G.L. Grady and E.F. Healy, *Organometallics, 6* (1987) 186.
19 M.J.S. Dewar, E.G. Zoebisch, E.F. Healy and J.J.P. Stewart, *J. Am. Chem. Soc., 107* (1985) 3902.
20 Ge-parameters: M.J.S. Dewar and C. Jie, *Organometallics, 8* (1989) 1544.
21 W. Thiel, program MNDO91, version 3.2.
22 A.J. Holder and C.W. Earley, *Organometallics, 11* (1992) 4350.

23 G. Trinquier, J.C. Barthelat and J. Satgé, *J. Am. Chem. Soc., 104* (1982) 5931.
24 K. Balasubramanian, *J. Chem. Phys., 89* (1988) 5731.
25 J.F. Harrison, R.C. Liedtke and J.F. Lieberman, *J. Am. Chem. Soc., 101* (1979) 7162.
26 S.P. So, *J. Phys. Chem., 95* (1991) 10658.
27 M. Benavides-Garcia and K. Balasubramanian, *J. Chem. Phys., 97* (1992) 7537.
28 N. Wiberg, K. Schurz, G. Reber and G. Müller, *J. Chem. Soc., Chem. Commun.,* (1986) 591.
29 C. Glidewell, D. Lloyd, K.W. Lumbard and J.S. McKechnie, *J. Chem. Soc., Dalton Trans.,* (1987) 2981; H.G. Ang and F.K. Lee, *J. Chem. Soc., Chem. Commun.,* (1989) 310; A. Meller, G. Ossig, W. Maringgele, D. Stalke, R. Herbst-Irmer, S. Freitag and G.M. Sheldrick, *J. Chem. Soc., Chem. Commun.,* (1991) 1123.
30 R.S. Grev and H.F. Schaefer, *Organometallics, 11* (1992) 3489.
31 M.W. Schmidt, P.N. Truong and M.S. Gordon, *J. Am. Chem. Soc., 109* (1987) 5217.
32 R.S. Grev, H.F. Schaefer and K.M. Baines, *J. Am. Chem. Soc., 112* (1990) 9458.
33 B.T. Luke, J.A. Pople, M.B. Krogh-Jespersen, Y. Apeloig, M. Karni, J. Chandrasekhar and P.v.R. Schleyer, *J. Am. Chem. Soc., 108* (1986) 270.
34 D. Smith, *Chem. Rev., 92* (1992) 1473.
35 R. Preuss, R.J. Buenker and S.D. Peyerimhoff, *J. Mol. Structure (THEOCHEM), 49* (1978) 171.
36 N. Goldberg, M. Iraqi, J. Hrusak and H. Schwarz, *Int. J. Mass Spectr. Ion Processes, 125* (1993) 267.
37 G. Winnewisser, A.G. Maki and D.R. Johnson, *J. Mol. Spectrosc., 39* (1971) 149.
38 W. Hehre, L. Radom, P.v.R. Schleyer and J.A. Pople, *Ab Initio Molecular Orbital Theory,* John Wiley, New York, 1986, p. 224f.
39 C. Heinemann, *Diploma thesis*, Technische Universität München, 1993.
40 G.S. Hammond, *J. Am. Chem. Soc., 77* (1955) 334.